INTERNATIONAL JOURNAL OF
NUMERICAL ANALYSIS AND MODELING
Volume 23, Number 3, Pages 442–459

doi: 10.4208/ijnam2026-1019

A HIGH-ORDER MIXED FINITE ELEMENT METHOD FOR SECOND ORDER ELLIPTIC EQUATIONS ON CURVED DOMAIN WITH BOUNDARY VALUE CORRECTIONS

YONGLI HOU[1], YI LIU[2,*], AND TENGJIN ZHAO[2]

Abstract. This paper presents a boundary corrections mixed finite element method for second order elliptic equations with the non-homogeneous Neumann boundary condition on curved domains. A key feature of the boundary value corrections is the shift from the true boundary to a surrogate boundary, which avoids numerical integration formula on curved elements. We consider the high-order Raviart-Thomas element (RT_k) of degree $k \geq 1$ on triangular meshes, achieving an $O(h^{k+1/2})$ convergence in the L^2-norm estimate for the velocity field and an $O(h^k)$ convergence in the H^1-norm estimate for the pressure. Finally, numerical experiments validate our theoretical results.

Key words. Mixed finite element method, boundary value corrections, Neumann boundary condition, curved domain.

1. Introduction

Many practical problems arising in science and engineering often involve domains with curved boundaries. For the domain Ω with curved boundaries, the geometric error between the curved boundary Γ and the approximating boundary Γ_h leads to a loss of accuracy for high-order elements [33, 34]. There are two main strategies to address this issue. Both the isoparametric finite element method [21, 27] and the isogeometric analysis [16, 23] aim to reduce the geometric error without modifying the variational form. The second strategy is the boundary value correction method [7], which directly solves on a polygonal approximation domain Ω_h, and focuses on a modified variational formulation. We also mention that there are other approaches such as the discontinuous Galerkin method [14, 15], the shifted boundary method [2, 29], the cut finite element method (cutFEM) with boundary value correction [11], the cut-cell finite element method [30], etc.

In this paper, we consider the mixed finite method (MFEM) for second order elliptic problems with non-homogeneous Neumann boundary conditions on curved domains. Although analysis of discretizations in the primal formulation on curved domains has long been widely recognized, the research of the mixed formulation is relatively rare. In the context of the mixed finite element method, Neumann boundary conditions become essential. A subtlety emerges in that the Neumann boundary condition entails the outward normal vector on the boundary, which is different on Γ and Γ_h. To the best of our knowledge, such a problem, as well as subsequent MFEM error analysis on curved domains was first studied by Bertrand et al. [3, 4] for the Raviart-Thomas element in 2014. Later, they extended the analysis to parametric Raviart-Thomas elements in [5]. However, in [3, 4, 5], a homogeneous Neumann boundary was considered and enforced in the discrete space. In [17, 12], concerning the study on polygonal domain, authors used penalty method

---

Received by the editors on October 8, 2024 and accepted on September 30, 2025.
2000 *Mathematics Subject Classification.* 65N15, 65N30.

*Corresponding author.

to weakly imposes the Neumann boundary conditions in the weak formulation. One of the purposes of our works is to research the possibility of weakening nonhomogeneous Neumann curved boundary conditions. It seems that one only needs to apply the penalty method to curved boundary. However, one also has to be careful about the difference of the outward normal vector between Γ and Γ_h.

This paper adopts the boundary value correction technique on curved boundary, where Taylor expansion is used to transfer the boundary condition from curved boundary to polygonal approximation boundary. In view of the differences in outward normal vector between Γ and Γ_h, we introduce a map to connect Γ and Γ_h and then utilize the penalty method to weakly impose the Neumann boundary. To our knowledge, the best error results of MFEM for second order elliptic with nonhomogeneous Neumann boundary is $O(h^k)$ for the velocity field in [31]; their work used the cutFEM to integrate directly on curved regions. We improve the error rates to $O(h^{k+1/2})$ and do not involve the curved elements. Furthermore, this work includes a rigorous analysis of the loss of approximation accuracy for high-order elements.

This paper is organized as follows. In section 2, we introduce some notations and preliminaries; In section 3, we describe the model problem and introduce the boundary value correction method; In section 4, we establish the discrete space and variational form and analyze its well-posedness; In section 5, the energy error estimate and the L^2 error estimate are proved; In section 6, we present several numerical experiments to verify the theoretical results; we conclude in 7 with our findings.

2. Notations and preliminaries

Throughout this paper, let Ω be a connected open set in $\mathbb{R}^2$ with Lipschitz continuous boundary Γ. We assume that Ω is approximated by a polygonal domain Ω_h and denote by Γ_h the boundary of Ω_h. Let $\mathcal{T}_h$ denote a family of triangular meshes for Ω_h. We require that all the vertices of $\mathcal{T}_h$ lying on Γ_h also lie on Γ, ensuring $\mathcal{T}_h$ is a body-fitted triangular partition of Ω. For each $K \in \mathcal{T}_h$, let $h_K = \mathrm{diam(K)}$ and $h = \max_{K\in\mathcal{T}_h} h_K$. We assume the mesh is shape-regular; that is, there exists a constant $\sigma > 0$, independent of h, such that $\max_{K\in\mathcal{T}_h} \frac{h_K}{\rho_K} \leq \sigma$, where ρ_K is the diameter of the largest ball inscribed in K. Furthermore, we assume that the mesh is quasi-uniform; that is, there exists $\tau > 0$, independent of h, such that $\min_{K\in\mathcal{T}_h} h_K \geq \tau h$. Let $\mathcal{E}_h$ denote the set of all edges in $\mathcal{T}_h$. Define $\mathcal{E}_h^o$ as the set of all interior edges and $\mathcal{E}_h^b = \mathcal{E}_h \setminus \mathcal{E}_h^o$. Denote by $\mathcal{T}_h^b$ all mesh elements containing at least one edge in $\mathcal{E}_h^b$ and $\mathcal{T}_h^o = \mathcal{T}_h \setminus \mathcal{T}_h^b$. Let e be an interior edge shared by two elements K_1 and K_2, we define the jump $[\cdot]$ on e for scalar functions q as follows:

$$[q] = q|_{K_1} - q|_{K_2}.$$

We adopt standard definitions for the Sobolev spaces as presented in [10]. Let $H^m(S)$, for $m \in \mathbb{R}$ and $S \subset \mathbb{R}^2$ be the usual Sobolev space with associated norm $\|\cdot\|_{m,S}$ and seminorm $|\cdot|_{m,S}$. When $m = 0$, the space $H^0(S)$ coincides with the square integrable space $L^2(S)$. We define

$$H^m(\mathcal{T}_h) := \prod_{K\in\mathcal{T}_h} H^m(K)$$

with seminorm

$$|\cdot|_{m,\mathcal{T}_h} := (\sum_{K\in\mathcal{T}_h} |\cdot|_{m,K}^2)^{1/2}.$$

We denote $\boldsymbol{H}^m(S)$ and $\boldsymbol{H}^m(\mathcal{T}_h)$ as representing the corresponding vector spaces.

We denote $L_0^2(S)$ as the mean value free subspace of $L^2(S)$. For $m \geq 0$, the above notation extends to a portion $s \subset \Gamma$ or $s \subset \Gamma_h$. For example, let $\|\cdot\|_{m,s}$ be the Sobolev norm on s. Denote by $(\cdot,\cdot)_S$ the L^2 inner-product on $S \subset \mathbb{R}^2$, and by $\langle\cdot,\cdot\rangle_s$ the duality pair on $s \subset \Gamma$ or $s \subset \Gamma_h$. Finally, all the above-defined notations can be easily extended to vector spaces using the standard product. Moreover,

$$H(\mathrm{div}, S) = \{\boldsymbol{v} \in \boldsymbol{L}^2(S) : \mathrm{div}\,\boldsymbol{v} \in L^2(S)\}.$$

The norm in $H(\mathrm{div}, S)$ is defined by

$$\|\boldsymbol{v}\|_{H(\mathrm{div},S)} = (\|\boldsymbol{v}\|_{0,S}^2 + \|\mathrm{div}\,\boldsymbol{v}\|_{0,S}^2)^{1/2}.$$

We will also use the notation

$$M_k(\boldsymbol{v}) = \max_{|\alpha|\leq k} \sup_{x\in\Omega_h} |D^\alpha \boldsymbol{v}(x)|.$$

In the remainder of the paper, we use the notation $\lesssim$ to denote less than or equal to up to a constant and the analogous notation $\gtrsim$ to denote greater than or equal to up to a constant.

Hereafter, we collect some well-known inequalities that are used in this paper.

Lemma 2.1. *(Trace Inequality* [10]*). For any $K \in \mathcal{T}_h$ and $v \in H^1(K)$, we have*

$$\|v\|_{0,\partial K} \lesssim h_K^{-1/2}\|v\|_{0,K} + h_K^{1/2}|v|_{1,K}.$$

Lemma 2.2. *(Poincaré-Friedrichs inequality* [9]*). For any $v \in H^1(\mathcal{T}_h)$, one gets*

$$\|v\|_{0,\Omega_h}^2 \lesssim \sum_{K\in\mathcal{T}_h} |v|_{1,K}^2 + \sum_{e\in\mathcal{E}_h^o} h^{-2}\left(\int_e [v]\ \mathrm{d}s\right)^2 + \left(\int_{\Omega_h} v\ \mathrm{d}x\right)^2.$$

Lemma 2.3. *(Inverse Inequality* [10]*). For any $K \in \mathcal{T}_h$ and $q \in P_j(K)$, $0 \leq m \leq j$, we have*

$$|q|_{j,K} \lesssim h_K^{m-j}|q|_{m,K}.$$

3. Model problem and the boundary value correction method

In this section, we briefly introduce the model problem and the boundary value correction method [7]. Consider the Poisson's equation in its mixed form: Given $f \in L^2(\Omega), g_N \in H^{-1/2}(\Gamma)$, find functions $\boldsymbol{u}$ and p such that

$$\begin{aligned} \boldsymbol{u} &= -\nabla p, && \text{in}\,\Omega, \\ \mathrm{div}\,\boldsymbol{u} &= f, && \text{in}\,\Omega, \\ \boldsymbol{u}\cdot\mathbf{n} &= g_N, && \text{on}\,\Gamma, \end{aligned} \tag{1}$$

where $\mathbf{n}$ denotes the unit outward normal on Γ. Problem (1) is well-posed as long as the following compatibility condition holds:

$$\int_\Omega f\ \mathrm{d}x = \int_\Gamma g_N\ \mathrm{d}s. \tag{2}$$

To shift the boundary date from Γ to Γ_h, we assume that there exists a map $M_h : \Gamma_h \to \Gamma$ defined as follows

$$M_h(\boldsymbol{x}_h) := \boldsymbol{x}_h + \delta_h(\boldsymbol{x}_h)\boldsymbol{\nu}_h(\boldsymbol{x}_h), \tag{3}$$

as shown in Fig. 1(b), where $\boldsymbol{\nu}_h$ is a unit vector pointing from $\boldsymbol{x}_h \in \Gamma_h$ to $M_h(\boldsymbol{x}_h) \in \Gamma$ and $\delta_h(\boldsymbol{x}_h) = |M_h(\boldsymbol{x}_h) - \boldsymbol{x}_h|$. Denote by $\boldsymbol{x} := M_h(\boldsymbol{x}_h)$ and by $\widetilde{\mathbf{n}} := \mathbf{n}\circ M_h$. As shown in [11], we have

$$\delta = \sup_{\boldsymbol{x}_h\in\Gamma_h} \delta_h(\boldsymbol{x}_h) \lesssim h^2, \qquad \|\widetilde{\mathbf{n}} - \mathbf{n}_h\|_{L^\infty(\Gamma_h)} \lesssim h, \tag{4}$$

where $\mathbf{n}_h$ denotes the unit outward normal on Γ_h.

Remark 3.1. *In this paper, we do not specify the map M_h. We only require that the distance function $\delta_h(\boldsymbol{x}_h)$ satisfies (4). Various definitions of the transfer direction ν_h (and consequently the mapping M_h) have been proposed in the literature, such as defining $\boldsymbol{\nu}_h$ as the unit outward normal vector $\mathbf{n}$ on Γ (as in* [1, 2]*), the unit outward normal vector $\mathbf{n}_h$ on Γ_h (as in* [7, 8]*) or other variants introduced in* [19, 20].

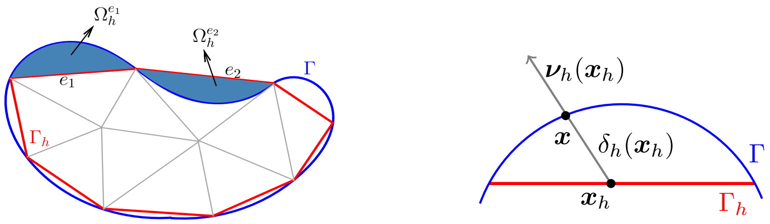

(a) (b)

FIGURE 1. (a). The true boundary Γ (blue curve), the approximated boundary Γ_h (red lines) and the typical region $\cup_{e\in\mathcal{E}_h^b}\Omega_h^e$ bounded by Γ and Γ_h. (b). The distance $\delta_h(\boldsymbol{x}_h)$ and the unit vector $\boldsymbol{\nu_h}$ to Γ_h.

Assuming $\boldsymbol{v}$ is sufficiently smooth in the strip between Γ and Γ_h to admit an m-th order Taylor expansion pointwise

$$\boldsymbol{v}(M_h(\boldsymbol{x}_h)) = \sum_{j=0}^{m} \frac{\delta_h^j(\boldsymbol{x}_h)}{j!} \partial_{\boldsymbol{\nu}_h}^j \boldsymbol{v}(\boldsymbol{x}_h) + R^m\boldsymbol{v}(\boldsymbol{x}_h), \qquad \text{on}\, \Gamma_h,$$

where $\partial_{\boldsymbol{\nu}_h}^j$ is the j-th partial derivative in the $\boldsymbol{\nu}_h$ direction, and the remainder $R^m\boldsymbol{v}(\boldsymbol{x}_h)$ satisfies

$$|R^m\boldsymbol{v}(\boldsymbol{x}_h)| = o(\delta^m).$$

For notational convenience, we define

$$T^m\boldsymbol{v} := \sum_{j=0}^{m} \frac{\delta_h^j(\boldsymbol{x}_h)}{j!} \partial_{\boldsymbol{\nu}_h}^j \boldsymbol{v}(\boldsymbol{x}_h), \quad T_1^m\boldsymbol{v} := \sum_{j=1}^{m} \frac{\delta_h^j(\boldsymbol{x}_h)}{j!} \partial_{\boldsymbol{\nu}_h}^j \boldsymbol{v}(\boldsymbol{x}_h). \tag{5}$$

Both $T^m\boldsymbol{v}$ and $T_1^m\boldsymbol{v}$ are functions defined on Γ_h. We denote $\widetilde{\boldsymbol{v}}(\boldsymbol{x}_h) := \boldsymbol{v}\circ M_h(\boldsymbol{x}_h)$, which is also a function on Γ_h. Thus, we have

$$T^m\boldsymbol{v} - \widetilde{\boldsymbol{v}} = -R^m\boldsymbol{v}. \tag{6}$$

For any $e\in\mathcal{E}_h^b$, by choosing local coordinates (ξ,η), we define $\Omega_h^e := \{(\xi,0) : 0\le\xi\le h_e\}$ with the condition that $\eta>0$ in Ω_h^e (See Fig. 1(a)). We present the following three lemmas.

Lemma 3.1. *(see Lemma 1 in* [8]*). For any $e\in\mathcal{E}_h^b$ and $\boldsymbol{v}\in\boldsymbol{H}^1(\Omega\cup\Omega_h)$, one gets*

$$\|\boldsymbol{v}-\widetilde{\boldsymbol{v}}\|_{0,e}^2 \lesssim \delta_h\|\nabla\boldsymbol{v}\|_{0,\Omega_h^e}^2.$$

Lemma 3.2. *(cf.* [8]*). For each $e\in\mathcal{E}_h^b$ and $v\in H^1(\Omega\cup\Omega_h)$, one has*

$$\|v\|_{0,\Omega_h^e} \lesssim \delta_h^{1/2}\|v\|_{0,\widetilde{e}} + \delta_h\|\nabla v\|_{0,\Omega_h^e}. \tag{7}$$

Moreover, when $v|_{\partial\Omega}=0$, one has

$$\|v\|_{0,\Omega_h^e} \lesssim \delta_h\|v\|_{1,\Omega_h^e}. \tag{8}$$

Lemma 3.3. *(cf. [28]). For $K \in \mathcal{T}_h^b$ and $q \in P_j(K)$, one has*

$$\sum_{e \subset \partial K \cap \Gamma_h} \|q\|_{0,\Omega_h^e}^2 \lesssim h_K \|q\|_{0,K}^2.$$

4. The finite element discretization

This section introduces the discrete space and a variational formulation. Then, we analyze the well-posedness of the discrete problem. Let $k \geq 1$ be a given integer. We define the discrete spaces V_h and Q_h as follows:

$$\begin{aligned} V_h &= \{\boldsymbol{v}_h \in H(\mathrm{div}, \Omega_h) : \boldsymbol{v}_h|_K \in RT_k(K), K \in \mathcal{T}_h\}, \\ Q_h &= \{q_h \in L^2(\Omega_h) : q_h|_K \in P_k(K), K \in \mathcal{T}_h\}, \end{aligned}$$

where $RT_k(K) := \boldsymbol{P}_k(K) \oplus \boldsymbol{x} P_k(K)$, with $P_k(K)$ denoting the space of polynomials on K with degree less than or equal to k, and $\boldsymbol{P}_k(K)$ representing the corresponding vector space. We denote $Q_{0h} := Q_h \cap L_0^2(\Omega_h)$.

For any $K \in \mathcal{T}_h$, we define the local interpolation operator $I_K : \boldsymbol{H}^s(K) \to RT_k(K), s > 1/2$, utilizing the degrees of freedom (dofs.) of Raviart-Thomas finite element [18].

$$(9) \qquad \begin{cases} \langle I_K \boldsymbol{v}_h \cdot \mathbf{n}_h, \phi_k \rangle_e = \langle \boldsymbol{v}_h \cdot \mathbf{n}_h, \phi_k \rangle_e, & \forall\, \phi_k \in P_k(e), \forall\, e \subset \partial K, \\ (I_K \boldsymbol{v}_h, \boldsymbol{\psi}_{k-1})_K = (\boldsymbol{v}_h, \boldsymbol{\psi}_{k-1})_K, & \forall\, \boldsymbol{\psi}_{k-1} \in \boldsymbol{P}_{k-1}(K). \end{cases}$$

Define the L^2-orthogonal projection $\Pi_k^0 : L^2(\Omega_h) \to Q_h$ such that for any $K \in \mathcal{T}_h$, the restriction $\Pi_k^{0,K} := \Pi_k^0|_K$ satisfies

$$(\Pi_k^{0,K} \phi, q_h)_K = (\phi, q_h)_K, \qquad \forall\, q_h \in Q_h.$$

For every $e \in \mathcal{E}_h$, let $\Pi_k^{0,e}$ denote the L^2-orthogonal projection onto $P_k(e)$.

Next, we state the approximation results of the nodal interpolant and L^2-orthogonal projections. The derivation of the following results is standard [22] and [10].

Lemma 4.1. *(cf. [22]). Let m and k be nonnegative integers such that $0 \leq m \leq k+1$. For any $\boldsymbol{v} \in \boldsymbol{H}^{k+1}(K)$, we have*

$$|\boldsymbol{v} - I_K \boldsymbol{v}|_{m,K} \lesssim h^{k-m+1} |\boldsymbol{v}|_{k+1,K}.$$

Lemma 4.2. *(cf. [10]). Let m and k be nonnegative integers such that $0 \leq m \leq k+1$. For any $v \in H^{k+1}(K)$ and $w \in H^{k+1}(e), e \subset \partial K$, one gets*

$$\begin{aligned} |v - \Pi_k^{0,K} v|_{m,K} &\lesssim h^{k-m+1} |v|_{k+1,K}, \\ |w - \Pi_k^{0,e} w|_{m,e} &\lesssim h^{k-m+1} |w|_{k+1,e}. \end{aligned}$$

Lemma 4.3. *(cf. [32]). Let Ω be a Lipschitz domain in $\mathbb{R}^2$ and $s \in \mathbb{R}$, with $s \geq 0$. For each $v \in H^s(\Omega)$, there exists an extension operator $E : H^s(\Omega) \to H^s(\mathbb{R}^2)$ such that*

$$Ev|_\Omega = v, \quad \|Ev\|_{s,\mathbb{R}^2} \lesssim \|v\|_{s,\Omega},$$

where the hidden constant depends on s but does not depend on the diameter of Ω. Additionally, we have

$$\|Ev\|_{s,\Omega_h} \leq \|Ev\|_{s,\mathbb{R}^2} \lesssim \|Ev\|_{s,\Omega}.$$

For brevity, we will also denote extended functions by $v^E = Ev$ and $f^E = Ef$ on $\mathbb{R}^2$.

4.1. A variational formulation. Before deriving a weak formulation, it's pointed out that $\boldsymbol{u}^E + \nabla p^E$, $\operatorname{div} \boldsymbol{u}^E - f^E$ are not generally equal to zero on $\Omega_h \backslash \Omega$ when $\Omega_h \nsubseteq \Omega$.

Next, we multiply the first equation of (1) by an arbitrary $\boldsymbol{v}_h \in V_h$ and integrate over Ω_h. This leads to the following result:

$$(\boldsymbol{u}^E, \boldsymbol{v}_h)_{\Omega_h} - (p^E, \operatorname{div} \boldsymbol{v}_h)_{\Omega_h} + \sum_{e \in \mathcal{E}_h^b} \langle \boldsymbol{v}_h \cdot \mathbf{n}_h, p^E \rangle_e = (\boldsymbol{u}^E + \nabla p^E, \boldsymbol{v}_h)_{\Omega_h}, \tag{10}$$

where we have used the fact that $\boldsymbol{v}_h \in V_h \subset H(\mathrm{div})$ implies that $\boldsymbol{v}_h \cdot \mathbf{n}_h$ is continuous across each interior edge. Next, by (6), one has

$$(T^k \boldsymbol{u}^E + R^k \boldsymbol{u}^E) \cdot \widetilde{\mathbf{n}} = \widetilde{g}_N, \qquad \text{on } \Gamma_h, \tag{11}$$

where $\widetilde{g}_N$ is a pull-back of the Neumann boundary data g_N from Γ to Γ_h. Then, the equality (10) can be rewritten as

$$\begin{aligned}(\boldsymbol{u}^E, \boldsymbol{v}_h)_{\Omega_h} &+ \sum_{e \in \mathcal{E}_h^b} \langle h_K^{-1} T^k \boldsymbol{u}^E \cdot \widetilde{\mathbf{n}}, T^k \boldsymbol{v}_h \cdot \widetilde{\mathbf{n}} \rangle_e - (p^E, \operatorname{div} \boldsymbol{v}_h)_{\Omega_h} + \sum_{e \in \mathcal{E}_h^b} \langle \boldsymbol{v}_h \cdot \mathbf{n}_h, p^E \rangle_e \\ &= \sum_{e \in \mathcal{E}_h^b} \langle h_K^{-1} (\widetilde{g}_N - R^k \boldsymbol{u}^E \cdot \widetilde{\mathbf{n}}), T^k \boldsymbol{v}_h \cdot \widetilde{\mathbf{n}} \rangle_e + (\boldsymbol{u}^E + \nabla p^E, \boldsymbol{v}_h)_{\Omega_h}.\end{aligned}$$

The second equation of (1) can be derived by testing any $q_h \in Q_h$ over Ω_h

$$(\operatorname{div} \boldsymbol{u}^E, q_h)_{\Omega_h} - (f^E, q_h)_{\Omega_h} = (\operatorname{div} \boldsymbol{u}^E - f^E, q_h)_{\Omega_h},$$

where we also note that $f^E = (\operatorname{div} \boldsymbol{u})^E$, and $\operatorname{div} \boldsymbol{u}^E \neq (\operatorname{div} \boldsymbol{u})^E$ on $\Omega_h \backslash \Omega$.

To simplify the notation, for any u, $v \in V_h$, and $p \in Q_h$, we define the following bilinear forms

$$\begin{aligned} a_h(\boldsymbol{u}, \boldsymbol{v}) &: = (\boldsymbol{u}, \boldsymbol{v})_{\Omega_h} + \sum_{e \in \mathcal{E}_h^b} \langle h_K^{-1} T^k \boldsymbol{u} \cdot \widetilde{\mathbf{n}}, T^k \boldsymbol{v} \cdot \widetilde{\mathbf{n}} \rangle_e, \\ b_{h1}(\boldsymbol{v}, p) &: = -(\operatorname{div} \boldsymbol{v}, p)_{\Omega_h} + \sum_{e \in \mathcal{E}_h^b} \langle \boldsymbol{v} \cdot \mathbf{n}_h, p \rangle_e, \\ b_{h0}(\boldsymbol{v}, p) &: = -(\operatorname{div} \boldsymbol{v}, p)_{\Omega_h}. \end{aligned} \tag{12}$$

Define the discrete weak formulation: *Find* $(\boldsymbol{u}_h, p_h) \in V_h \times Q_{0h}$ *such that*

$$\begin{cases} a_h(\boldsymbol{u}_h, \boldsymbol{v}_h) + b_{h1}(\boldsymbol{v}_h, p_h) = \sum_{e \in \mathcal{E}_h^b} \langle h_K^{-1} \widetilde{g}_N, T^k \boldsymbol{v}_h \cdot \widetilde{\mathbf{n}} \rangle_e, & \forall \boldsymbol{v}_h \in V_h, \\ \qquad\qquad b_{h0}(\boldsymbol{u}_h, q_h) = -(f^E, q_h)_{\Omega_h}, & \forall q_h \in Q_{0h}. \end{cases} \tag{13}$$

The well-posedness of the continuous problem (1) requires the compatibility condition (2). However, the discrete problem handles compatibility differently. Specifically, the enforcement of the essential boundary condition $\boldsymbol{u} \cdot \mathbf{n} = g_N$ on Γ has been relaxed in formulation 13, eliminating the need for any explicit relationship between g_N^E and f^E. In Section 4.2, we have proved the existence of a unique solution to 13, confirming its inherent compatibility.

From an implementation perspective, the space Q_{0h} presents practical challenges for basis construction. Instead, we work directly with Q_h, which admits a more computationally tractable basis. This motivates our equivalent discrete formulation that preserves solution properties while being more implementation-friendly. Hence we introduce an equivalent discrete problem: *Find* $(\boldsymbol{u}_h, p_h) \in V_h \times Q_h$ *such that*

$$\left\{\begin{aligned} a_h(\boldsymbol{u}_h, \boldsymbol{v}_h) + b_{h1}(\boldsymbol{v}_h, p_h) &= \sum_{e\in\mathcal{E}_h^b} \langle h_K^{-1}\widetilde{g}_N, T^k\boldsymbol{v}_h \cdot \widetilde{\mathbf{n}}\rangle_e, && \forall \boldsymbol{v}_h \in V_h,\\ b_{h0}(\boldsymbol{u}_h, q_h) + \sum_{e\in\mathcal{E}_h^b} \langle \boldsymbol{u}_h \cdot \mathbf{n}_h, \bar{q}_h\rangle_e &= -(f^E - \overline{f^E}, q_h)_{\Omega_h}, && \forall q_h \in Q_h. \end{aligned}\right. \tag{14}$$

Lemma 4.4. *The systems (13) and (14) admit the same solution in* $V_h \times Q_{0h}$*.*

Proof. The space Q_h admits an orthogonal decomposition $Q_h = Q_{0h} \oplus \mathbb{R}$ with respect to the $L^2(\Omega_h)$ inner product. Through integration by parts, we immediately observe that $b_{h1}(\boldsymbol{v}_h, 1) = 0$ for all $\boldsymbol{v}_h \in V_h$. Consider now $q_h - \bar{q}_h \in Q_{0h}$ where $\bar{q}_h$ denotes the mean value component. The second equation in (13) yields for arbitrary $q_h \in Q_h$:

$$b_{h0}(\boldsymbol{u}_h, q_h - \bar{q}_h) = -(f^E, q_h - \bar{q}_h)_{\Omega_h},$$

organized as follows:

$$b_{h0}(\boldsymbol{u}_h, q_h) + \sum_{e\in\mathcal{E}_h^b} \langle \boldsymbol{u}_h \cdot \mathbf{n}_h, \bar{q}_h\rangle_e = -(f^E, q_h - \bar{q}_h)_{\Omega_h}$$

This establishes the second equation in (14), completing the proof. □

Provided that (13) is well-posed, the discrete problem (14) admits a solution, indicating that the associated linear system is "compatible". Nevertheless, the solution lacks uniqueness, as any pair $(\boldsymbol{u}_h, p_h + c)$ with $c \in \mathbb{R}$ equally satisfies the system. To deal with this case, one can add a constraint to the linear system to ensure that the solution stays in $V_h \times Q_{0h}$.

For any $\boldsymbol{v}_h \in V_h$ and $q_h \in Q_{0h}$, define two mesh-dependent norms as follows

$$\|\boldsymbol{v}_h\|_{0,h} = \left(\|\boldsymbol{v}_h\|_{0,\Omega_h}^2 + \sum_{e\in\mathcal{E}_h^b} \|h_K^{-1/2} T^k \boldsymbol{v}_h \cdot \widetilde{\mathbf{n}}\|_{0,e}^2\right)^{1/2},$$

$$\|q_h\|_{1,h} = \left(\sum_{K\in\mathcal{T}_h} \|\nabla q_h\|_{0,K}^2 + \sum_{e\in\mathcal{E}_h^o} h^{-1}\|[q_h]\|_{0,e}^2\right)^{1/2}.$$

4.2. Well-posedness. In this subsection, we discuss the well-posedness of the discrete problem (13). First, we list some relevant lemmas.

Lemma 4.5. *Under the assumption of (4), for any* $\boldsymbol{v}_h \in V_h$*, it holds that*

$$\sum_{e\in\mathcal{E}_h^b} \|h_K^{-1/2} T_1^m \boldsymbol{v}_h\|_{0,e}^2 \lesssim \|\boldsymbol{v}_h\|_{0,\Omega_h}^2, \tag{15}$$

$$\sum_{e\in\mathcal{E}_h^b} \|h_K^{-1/2} T^m \boldsymbol{v}_h\|_{0,e}^2 \lesssim h^{-2}\|\boldsymbol{v}_h\|_{0,\Omega_h}^2. \tag{16}$$

Proof. From the definition in (5), along with the trace and inverse inequalities from Lemmas 2.1 and 2.3, we obtain the proof of this lemma. □

Lemma 4.6. *For each* $\boldsymbol{v}_h \in V_h$ *and* $\phi \in \prod_{e\in\mathcal{E}_h^b} L^2(e)$*, we have*

$$\sum_{e\in\mathcal{E}_h^b} \langle \boldsymbol{v}_h \cdot \mathbf{n}_h, \phi\rangle_e \lesssim \left(\sum_{e\in\mathcal{E}_h^b} h\|\phi\|_{0,e}^2\right)^{1/2} \|\boldsymbol{v}_h\|_{0,h}.$$

Proof. By the definition in (5), notice that $\boldsymbol{v}_h = T^k\boldsymbol{v}_h - T_1^k\boldsymbol{v}_h$, one gets

$$\begin{aligned}\sum_{e\in\mathcal{E}_h^b}\langle \boldsymbol{v}_h\cdot\mathbf{n}_h,\phi\rangle_e &= \sum_{e\in\mathcal{E}_h^b}\left(\langle \boldsymbol{v}_h\cdot\widetilde{\mathbf{n}},\phi\rangle_e + \langle \boldsymbol{v}_h\cdot(\mathbf{n}_h-\widetilde{\mathbf{n}}),\phi\rangle_e\right)\\ &= \sum_{e\in\mathcal{E}_h^b}\left(\langle T^k\boldsymbol{v}_h\cdot\widetilde{\mathbf{n}},\phi\rangle_e - \langle T_1^k\boldsymbol{v}_h\cdot\widetilde{\mathbf{n}},\phi\rangle_e\right) + \sum_{e\in\mathcal{E}_h^b}\langle \boldsymbol{v}_h\cdot(\mathbf{n}_h-\widetilde{\mathbf{n}}),\phi\rangle_e.\end{aligned}$$

By the Schwarz inequality and (4), one has

$$\begin{aligned}&\sum_{e\in\mathcal{E}_h^b}\langle \boldsymbol{v}_h\cdot\mathbf{n}_h,\phi\rangle_e\\ &\le \sum_{e\in\mathcal{E}_h^b}\left(h_K^{-1/2}\|T^k\boldsymbol{v}_h\cdot\widetilde{\mathbf{n}}\|_{0,e} + h_K^{-1/2}\|T_1^k\boldsymbol{v}_h\cdot\widetilde{\mathbf{n}}\|_{0,e} + h_K^{1/2}\|\boldsymbol{v}_h\|_{0,e}\right)h_K^{1/2}\|\phi\|_{0,e}.\end{aligned}$$

Next, according to Lemma 4.5 and the inverse inequality, it is not hard to obtain

$$\begin{aligned}\sum_{e\in\mathcal{E}_h^b}\langle \boldsymbol{v}_h\cdot\mathbf{n}_h,\phi\rangle_e &\lesssim \left(\sum_{e\in\mathcal{E}_h^b}\|h_K^{-1/2}T^k\boldsymbol{v}_h\cdot\widetilde{\mathbf{n}}\|_{0,e}^2 + \|\boldsymbol{v}_h\|_{0,\Omega_h}^2\right)^{1/2}\left(\sum_{e\in\mathcal{E}_h^b}h\|\phi\|_{0,e}^2\right)^{1/2}\\ &\lesssim \left(\sum_{e\in\mathcal{E}_h^b}h\|\phi\|_{0,e}^2\right)^{1/2}\|\boldsymbol{v}_h\|_{0,h}.\end{aligned}$$

□

Corollary 4.1. *For any $\boldsymbol{v}_h\in V_h$ and $q_h\in Q_{0h}$, we have*

$$\sum_{e\in\mathcal{E}_h^b}\langle \boldsymbol{v}_h\cdot\mathbf{n}_h,q_h\rangle_e \lesssim \|\boldsymbol{v}_h\|_{0,h}\|q_h\|_{1,h}.$$

Proof. Replacing ϕ of Lemma 4.6 by q_h, it holds that

$$\sum_{e\in\mathcal{E}_h^b}\langle \boldsymbol{v}_h\cdot\mathbf{n}_h,q_h\rangle_e \lesssim \left(\sum_{e\in\mathcal{E}_h^b}h\|q_h\|_{0,e}^2\right)^{1/2}\|\boldsymbol{v}_h\|_{0,h}.$$

By the trace and inverse inequalities in Lemmas 2.1 and 2.3, we obtain

$$\sum_{e\in\mathcal{E}_h^b}\langle \boldsymbol{v}_h\cdot\mathbf{n}_h,q_h\rangle_e \lesssim \|\boldsymbol{v}_h\|_{0,h}\|q_h\|_{0,\Omega_h}. \tag{17}$$

Notice that $q_h\in Q_{0h}$, which implies $\int_{\Omega_h} q_h\,\mathrm{d}x = 0$. Thus, by the Poincaré-Friedrichs inequality in Lemma 2.2, yielding

$$\|q_h\|_{0,\Omega_h}^2 \lesssim \|q_h\|_{1,h}^2. \tag{18}$$

Substituting (18) into (17), we obtain the desired result. □

We are now in the position to state the main results of this subsection:

Lemma 4.7. *For any $\boldsymbol{u}_h,\boldsymbol{v}_h\in V_h$ and $q_h\in Q_{0h}$, one gets*

$$|a_h(\boldsymbol{u}_h,\boldsymbol{v}_h)| \le \|\boldsymbol{u}_h\|_{0,h}\|\boldsymbol{v}_h\|_{0,h},\qquad |a_h(\boldsymbol{v}_h,\boldsymbol{v}_h)| = \|\boldsymbol{v}_h\|_{0,h}^2, \tag{19}$$

$$|b_{h1}(\boldsymbol{v}_h,q_h)| \lesssim \|\boldsymbol{v}_h\|_{0,h}\|q_h\|_{1,h},\qquad |b_{h0}(\boldsymbol{v}_h,q_h)| \lesssim \|\boldsymbol{v}_h\|_{0,h}\|q_h\|_{1,h}. \tag{20}$$

Proof. From the definition of $\|\cdot\|_{0,h}$, it is evident to complete the proof of (19). Then, we only need to prove (20). By integration by parts and the Schwarz inequality, we obtain

$$\begin{aligned} b_{h1}(\boldsymbol{v}_h, q_h) &= -\sum_{K\in\mathcal{T}_h}(\operatorname{div}\boldsymbol{v}_h, q_h)_K + \sum_{e\in\mathcal{E}_h^b}\langle \boldsymbol{v}_h\cdot\mathbf{n}_h, q_h\rangle_e \\ &= \sum_{K\in\mathcal{T}_h}(\boldsymbol{v}_h, \nabla q_h)_K - \sum_{e\in\mathcal{E}_h^o}\langle \boldsymbol{v}_h\cdot\mathbf{n}_h, [q_h]\rangle_e \\ &\le \sum_{K\in\mathcal{T}_h}\|\boldsymbol{v}_h\|_{0,K}\|\nabla q_h\|_{0,K} + \sum_{e\in\mathcal{E}_h^o} h^{1/2}\|\boldsymbol{v}_h\cdot\mathbf{n}_h\|_{0,e}h^{-1/2}\|[q_h]\|_{0,e}, \end{aligned}$$

using the trace and inverse inequalities in Lemmas 2.1, 2.3, we get

$$h^{1/2}\|\boldsymbol{v}_h\cdot\mathbf{n}_h\|_{0,e} \le h^{1/2}\|\boldsymbol{v}_h\|_{0,e} \lesssim \|\boldsymbol{v}_h\|_{0,K_1\cup K_2}, \quad e\in\mathcal{E}_h^o,\ e = K_1\cap K_2. \tag{21}$$

Then

$$|b_{h1}(\boldsymbol{v}_h, q_h)| \lesssim \|\boldsymbol{v}_h\|_{0,h}\|q_h\|_{1,h}.$$

Similarly, by Corollary 4.1, the bound of $b_{h0}(\boldsymbol{v}_h, q_h)$ can be estimated as

$$\begin{aligned} |b_{h0}(\boldsymbol{v}_h, q_h)| &= |\sum_{K\in\mathcal{T}_h}(\boldsymbol{v}_h, \nabla q_h)_K - \sum_{e\in\mathcal{E}_h^o}\langle \boldsymbol{v}_h\cdot\mathbf{n}_h, [q_h]\rangle_e - \sum_{e\in\mathcal{E}_h^b}\langle \boldsymbol{v}_h\cdot\mathbf{n}_h, q_h\rangle_e| \\ &\lesssim \|\boldsymbol{v}_h\|_{0,h}\|q_h\|_{1,h} + |\sum_{e\in\mathcal{E}_h^b}\langle \boldsymbol{v}_h\cdot\mathbf{n}_h, q_h\rangle_e| \\ &\lesssim \|\boldsymbol{v}_h\|_{0,h}\|q_h\|_{1,h}. \end{aligned} \tag{22}$$

Thus, we complete the proof of this lemma. □

Lemma 4.8. *(Inf-Sup). For all $q_h \in Q_{0h}$, it holds that*

$$\sup_{\boldsymbol{v}_h\in V_h}\frac{b_{h1}(\boldsymbol{v}_h, q_h)}{\|\boldsymbol{v}_h\|_{0,h}} \gtrsim \|q_h\|_{1,h}, \qquad \sup_{\boldsymbol{v}_h\in V_h}\frac{b_{h0}(\boldsymbol{v}_h, q_h)}{\|\boldsymbol{v}_h\|_{0,h}} \gtrsim \|q_h\|_{1,h}.$$

Proof. For an arbitrary $q_h \in Q_{0h}$, we construct $\boldsymbol{v}_h$ using the degrees of freedom of the Raviart-Thomas space as follows:

$$\langle \boldsymbol{v}_h\cdot\mathbf{n}_h, \phi_k\rangle_e = -h^{-1}\langle[q_h], \phi_k\rangle_e, \qquad \forall\phi_k\in P_k(e), \forall\, e\in\mathcal{E}_h^o, \tag{23}$$

$$\langle \boldsymbol{v}_h\cdot\mathbf{n}_h, \phi_k\rangle_e = 0, \qquad \forall\phi_k\in P_k(e), \forall e\in\mathcal{E}_h^b, \tag{24}$$

$$(\boldsymbol{v}_h, \boldsymbol{\psi}_{k-1})_K = (\nabla q_h, \boldsymbol{\psi}_{k-1})_K, \qquad \forall\boldsymbol{\psi}_{k-1}\in \boldsymbol{P}_{k-1}(K), \forall\, K\in\mathcal{T}_h. \tag{25}$$

From reference [12], it is straightforward to obtain

$$b_{h1}(\boldsymbol{v}_h, q_h) = \|q_h\|_{1,h}^2, \qquad \|\boldsymbol{v}_h\|_{0,\Omega_h} \lesssim \|q_h\|_{1,h}. \tag{26}$$

Recalling the definition of $\|\cdot\|_{0,h}$, it suffices to prove the inequality

$$\sum_{e\in\mathcal{E}_h^b}\|h_K^{-1/2}T^k\boldsymbol{v}_h\cdot\widetilde{\mathbf{n}}\|_{0,e} \lesssim \|q_h\|_{1,h}.$$

Indeed, for each $e\in\mathcal{E}_h^b$ and $\boldsymbol{v}_h\in V_h$ implies $\boldsymbol{v}_h\cdot\mathbf{n}_h|_e \in P_k(e)$. Then, replacing ϕ_k of (24) with $\boldsymbol{v}_h\cdot\mathbf{n}_h$, we have

$$\boldsymbol{v}_h\cdot\mathbf{n}_h|_e = 0, \qquad \forall e\in\mathcal{E}_h^b. \tag{27}$$

Furthermore, by the triangle inequality, it has

$$\begin{aligned}&\sum_{e\in\mathcal{E}_h^b}\|h_K^{-1/2}T^k\boldsymbol{v}_h\cdot\widetilde{\mathbf{n}}\|_{0,e}^2\\ &\lesssim\sum_{e\in\mathcal{E}_h^b}h_K^{-1}(\|T^k\boldsymbol{v}_h\cdot\mathbf{n}_h\|_{0,e}^2+\sum_{e\in\mathcal{E}_h^b}h_K^{-1}\|T^k\boldsymbol{v}_h\cdot\widetilde{\mathbf{n}}-\mathbf{n}_h\|_{0,e}^2)\\ &\lesssim\sum_{e\in\mathcal{E}_h^b}h_K^{-1}(\|T_1^k\boldsymbol{v}_h\cdot\mathbf{n}_h\|_{0,e}^2+\|T^k\boldsymbol{v}_h\cdot(\widetilde{\mathbf{n}}-\mathbf{n}_h)\|_{0,e}^2).\end{aligned}\tag{28}$$

Applying Lemma 4.5 and (4), we obtain

$$\sum_{e\in\mathcal{E}_h^b}h_K^{-1}\|T_1^k\boldsymbol{v}_h\cdot\mathbf{n}_h\|_{0,e}^2\lesssim\|\boldsymbol{v}_h\|_{0,\Omega_h}^2,\tag{29}$$

and

$$\begin{aligned}\sum_{e\in\mathcal{E}_h^b}h_K^{-1}\|T^k\boldsymbol{v}_h\cdot(\widetilde{\mathbf{n}}-\mathbf{n}_h)\|_{0,e}^2&\lesssim h^{-2}\|\boldsymbol{v}_h\|_{0,\Omega_h}^2\|\widetilde{\mathbf{n}}-\mathbf{n}_h\|_{L^\infty(\Gamma_h)}^2\\ &\lesssim\|\boldsymbol{v}_h\|_{0,\Omega_h}^2.\end{aligned}\tag{30}$$

Finally, combining (26)-(30), we establish the first inequality of this lemma.

Similarly to the estimate of $b_{h1}(\boldsymbol{v}_h,q_h)$, by integration by parts and (27), one gets

$$\begin{aligned}b_{h0}(\boldsymbol{v}_h,q_h)&=\sum_{K\in\mathcal{T}_h}(\boldsymbol{v}_h,\nabla q_h)_K-\sum_{e\in\mathcal{E}_h^o}\langle\boldsymbol{v}_h\cdot\mathbf{n}_h,[q_h]\rangle_e\\ &=\sum_{K\in\mathcal{T}_h}\|\nabla q_h\|_{0,K}^2+\sum_{e\in\mathcal{E}_h^o}h^{-1}\|[q_h]\|_{0,e}^2=\|q_h\|_{1,h}^2.\end{aligned}$$

Thus, we complete the proof of this lemma. ☐

According to the Brezzi theorem, the discrete problem (13) admits a unique solution.

5. Error analysis

In this section, we will estimate the errors in mesh-dependent norm and L^2-norm. The stability estimates of $a_h(\cdot,\cdot),b_{h0}(\cdot,\cdot)$ and $b_{h1}(\cdot,\cdot)$ imply

$$\|\boldsymbol{\sigma}_h,\zeta_h\|_H\lesssim\sup_{(\boldsymbol{v}_h,q_h)\in V_h\times Q_{0h}}\frac{B_h((\boldsymbol{\sigma}_h,\zeta_h),(\boldsymbol{v}_h,q_h))}{\|\boldsymbol{v}_h,q_h\|_H},\qquad\forall\,(\boldsymbol{\sigma}_h,\zeta_h)\in V_h\times Q_{0h},\tag{31}$$

where

$$\begin{aligned}B_h((\boldsymbol{\sigma}_h,\zeta_h),(\boldsymbol{v}_h,q_h))&:=a_h(\boldsymbol{\sigma}_h,\boldsymbol{v}_h)+b_{h1}(\boldsymbol{v}_h,\zeta_h)+b_{h0}(\boldsymbol{\sigma}_h,q_h),\\ \|\boldsymbol{\sigma}_h,\zeta_h\|_H&:=(\|\boldsymbol{\sigma}_h\|_{0,h}^2+\|\zeta_h\|_{1,h}^2)^{1/2}.\end{aligned}$$

To obtain the error estimates, we need the following lemma.

Lemma 5.1. *Assume that $\boldsymbol{w}\in W^{k+1,\infty}(\Omega)\cap\boldsymbol{H}^{r+1}(\Omega)$, $\boldsymbol{w}^E$ is the extended function of $\boldsymbol{w}$. For any $\boldsymbol{v}_h\in V_h$, the interpolation operator $\boldsymbol{w}_I$ of $\boldsymbol{w}^E$ satisfies*

$$\begin{aligned}&\sum_{e\in\mathcal{E}_h^b}\langle h_K^{-1}T^k(\boldsymbol{w}^E-\boldsymbol{w}_I)\cdot\widetilde{\mathbf{n}},T^k\boldsymbol{v}_h\cdot\widetilde{\mathbf{n}}\rangle_e\\ &\lesssim\left(h^{k+1/2}\|\boldsymbol{w}^E\|_{k+1,\infty,\Omega_h}+h^{r+1}|\boldsymbol{w}^E|_{r+1,\Omega_h}\right)\|\boldsymbol{v}_h\|_{0,h}.\end{aligned}$$

Proof. By applying the Schwarz inequality and (4), we infer that

$$
\begin{aligned}
&\sum_{e\in\mathcal{E}_h^b}\langle h_K^{-1}T^k(\boldsymbol{w}^E-\boldsymbol{w}_I)\cdot\widetilde{\mathbf{n}},T^k\boldsymbol{v}_h\cdot\widetilde{\mathbf{n}}\rangle_e\\
=&\sum_{e\in\mathcal{E}_h^b}h_K^{-1}\langle T^k(\boldsymbol{w}^E-\boldsymbol{w}_I)\cdot\mathbf{n}_h+T^k(\boldsymbol{w}^E-\boldsymbol{w}_I)\cdot(\widetilde{\mathbf{n}}-\mathbf{n}_h),T^k\boldsymbol{v}_h\cdot\widetilde{\mathbf{n}}\rangle_e\\
\lesssim&\sum_{e\in\mathcal{E}_h^b}h_K^{-1}\bigg(\langle(\boldsymbol{w}^E-\boldsymbol{w}_I)\cdot\mathbf{n}_h+T_1(\boldsymbol{w}^E-\boldsymbol{w}_I)\cdot\mathbf{n}_h,T^k\boldsymbol{v}_h\cdot\widetilde{\mathbf{n}}\rangle_e\\
&\quad+\|\widetilde{\mathbf{n}}-\mathbf{n}_h\|_{\infty,\Gamma_h}\|T^k(\boldsymbol{w}^E-\boldsymbol{w}_I)\|_{0,e}\|T^k\boldsymbol{v}_h\cdot\widetilde{\mathbf{n}}\|_{0,e}\bigg)\\
\lesssim&\bigg(\sum_{e\in\mathcal{E}_h^b}h^{-1}(\|(\boldsymbol{w}^E-\boldsymbol{w}_I)\cdot\mathbf{n}_h\|_{0,e}^2+\|T_1^k(\boldsymbol{w}^E-\boldsymbol{w}_I)\|_{0,e}^2\\
&\quad+h^2\|T^k(\boldsymbol{w}^E-\boldsymbol{w}_I)\|_{0,e}^2)\bigg)^{1/2}\|\boldsymbol{v}_h\|_{0,h}.
\end{aligned}
$$

From the definition of interpolation, we observe that $\boldsymbol{w}_I\cdot\mathbf{n}_h|_e=\Pi_k^{0,e}(\boldsymbol{w}\cdot\mathbf{n}_h)$. Then, by Lemma 4.1, we deduce that

$$
\begin{aligned}
\sum_{e\in\mathcal{E}_h^b}h^{-1}\|(\boldsymbol{w}^E-\boldsymbol{w}_I)\cdot\mathbf{n}_h\|_{0,e}^2&\lesssim h^{2k+1}\sum_{e\in\mathcal{E}_h^b}\|\boldsymbol{w}^E\cdot\mathbf{n}_h\|_{k+1,e}^2\\
&\lesssim h^{2k+1}\sum_{e\in\mathcal{E}_h^b}|e|\|\boldsymbol{w}^E\|_{k+1,\infty,e}^2\\
&\lesssim h^{2k+1}\|\boldsymbol{w}^E\|_{k+1,\infty,\Omega_h}^2.
\end{aligned}
$$

By the trace inequality in Lemmas 2.1 and 4.1, we have

$$
\sum_{e\in\mathcal{E}_h^b}h^{-1}(\|T_1^k(\boldsymbol{w}^E-\boldsymbol{w}_I)\|_{0,e}^2+h^2\|T^k(\boldsymbol{w}^E-\boldsymbol{w}_I)\|_{0,e}^2)\lesssim h^{2(r+1)}|\boldsymbol{w}^E|_{r+1,\Omega_h}^2.
$$

Combining the above, we complete the proof of this lemma. □

Theorem 5.1. *Assume that $\delta\lesssim h^2$. For any constants $r,t,l\geq 1$, let $(\boldsymbol{u},p)\in\boldsymbol{W}^{k+1,\infty}(\Omega)\cap\boldsymbol{H}^{\max\{r+1,\lceil l/2\rceil\}}(\Omega)\times H^{\max\{t+1,\lceil l/2\rceil\}}(\Omega)$ be the solution of problem (1) and $\boldsymbol{u}^E$, p^E are extended functions of $\boldsymbol{u}$ and p. Let $(\boldsymbol{u}_h,p_h)\in V_h\times Q_{0h}$ be the discrete solution of (13), $s:=\min\{r,t,k\}$, it holds that*

$$
\begin{aligned}
&\|\boldsymbol{u}_h-\boldsymbol{u}_I\|_{0,h}+\|p_h-p_I\|_{1,h}\\
\lesssim&h^{s+1}(|\boldsymbol{u}|_{r+1,\Omega}+|p|_{t+1,\Omega})+h^{k+1/2}\|\boldsymbol{u}^E\|_{k+1,\infty,\Omega_h}+\delta^{k+1}h^{-\frac{1}{2}}M_{k+1}(\boldsymbol{u}^E)\\
&+\delta^l\bigg(\|D^l(\boldsymbol{u}^E+\nabla p^E)\|_{0,\Omega_h\setminus\Omega}+\|D^l(\operatorname{div}\boldsymbol{u}^E-f^E)\|_{0,\Omega_h\setminus\Omega}\bigg),
\end{aligned}
$$

where $\boldsymbol{u}_I$ and p_I denote the interpolation and L^2 projection of $\boldsymbol{u}^E$ and p^E, respectively.

Proof. From (31), one has

$$
\|\boldsymbol{u}_h-\boldsymbol{u}_I,p_h-p_I\|_H\lesssim\sup_{(\boldsymbol{v}_h,q_h)\in V_h\times Q_{0h}}\frac{B_h((\boldsymbol{u}_h-\boldsymbol{u}_I,p_h-p_I),(\boldsymbol{v}_h,q_h))}{\|\boldsymbol{v}_h,q_h\|_H}. \tag{32}
$$

By adding and subtracting $\boldsymbol{u}^E$ and p^E, one obtains

$$\begin{aligned} &B_h((\boldsymbol{u}_h-\boldsymbol{u}_I,p_h-p_I),(\boldsymbol{v}_h,q_h))\\ &=a_h(\boldsymbol{u}_h-\boldsymbol{u}^E,\boldsymbol{v}_h)+b_{h1}(\boldsymbol{v}_h,p_h-p^E)+b_{h0}(\boldsymbol{u}_h-\boldsymbol{u}^E,q_h)\\ &\quad+a_h(\boldsymbol{u}^E-\boldsymbol{u}_I,\boldsymbol{v}_h)+b_{h1}(\boldsymbol{v}_h,p^E-p_I)+b_{h0}(\boldsymbol{u}^E-\boldsymbol{u}_I,q_h)\\ &:=E_R+E_h. \end{aligned}\tag{33}$$

By the primal problem (1), the discrete problem (13), along with equations (11) and (8), the consistency error is expressed as follows

$$\begin{aligned} E_R&=a_h(\boldsymbol{u}_h-\boldsymbol{u}^E,\boldsymbol{v}_h)+b_{h1}(\boldsymbol{v}_h,p_h-p^E)+b_{h0}(\boldsymbol{u}_h-\boldsymbol{u}^E,q_h)\\ &=\sum_{e\in\mathcal{E}_h^b}h^{-1}\langle\widetilde{g}_N-T^k\boldsymbol{u}^E\cdot\widetilde{\mathbf{n}},T^k\boldsymbol{v}_h\cdot\widetilde{\mathbf{n}}\rangle_e+(\boldsymbol{u}^E-\nabla p^E,\boldsymbol{v}_h)_{\Omega_h}\\ &\quad+(\operatorname{div}u^E-f^E,q_h)_{\Omega_h}\\ &\lesssim\delta^{k+1}h^{-1/2}M_{k+1}(\boldsymbol{u}^E)\|\boldsymbol{v}_h\|_{0,h}+\delta^l\bigg(\|D^l(\boldsymbol{u}^E+\nabla p^E)\|_{0,\Omega_h\setminus\Omega}\\ &\quad+\|D^l(\operatorname{div}\boldsymbol{u}^E-f^E)\|_{0,\Omega_h\setminus\Omega}\bigg)\|\boldsymbol{v}_h,q_h\|_H, \end{aligned}\tag{34}$$

where we have utilized $(\boldsymbol{u}^E-\nabla p^E)|_\Omega=0$ and $(\operatorname{div}\boldsymbol{u}^E-f^E)|_\Omega=0$. Next, we estimate the remaining approximation terms. From the definition of interpolation given in (9), it follows that

$$\begin{aligned} b_{h0}(\boldsymbol{u}^E-\boldsymbol{u}_I,q_h)&=-(\operatorname{div}(\boldsymbol{u}^E-\boldsymbol{u}_I),q_h)\\ &=\sum_{K\in\mathcal{T}_h}(\boldsymbol{u}^E-\boldsymbol{u}_I,\nabla q_h)_K-\sum_{K\in\mathcal{T}_h}\langle(\boldsymbol{u}^E-\boldsymbol{u}_I)\cdot\mathbf{n}_h,q_h\rangle_{\partial K}\\ &=0, \end{aligned}$$

and

$$\begin{aligned} b_{h1}(\boldsymbol{v}_h,p^E-p_I)&=-\sum_{K\in\mathcal{T}_h}(\operatorname{div}\boldsymbol{v}_h,p^E-p_I)_K+\sum_{e\in\mathcal{E}_h^b}\langle\boldsymbol{v}_h\cdot\mathbf{n}_h,p^E-p_I\rangle_e\\ &=\sum_{e\in\mathcal{E}_h^b}\langle\boldsymbol{v}_h\cdot\mathbf{n}_h,p^E-p_I\rangle_e. \end{aligned}$$

Thus, by rearranging the term E_h, we deduce

$$\begin{aligned} E_h&=a_h(\boldsymbol{u}^E-\boldsymbol{u}_I,\boldsymbol{v}_h)+b_{h1}(\boldsymbol{v}_h,p^E-p_I)+b_{h0}(\boldsymbol{u}^E-\boldsymbol{u}_I,q_h)\\ &=a_h(\boldsymbol{u}^E-\boldsymbol{u}_I,\boldsymbol{v}_h)+\sum_{e\in\mathcal{E}_h^b}\langle\boldsymbol{v}_h\cdot\mathbf{n}_h,p^E-p_I\rangle_e. \end{aligned}$$

By the Schwarz inequality and Lemmas 5.1, 4.1, we derive

$$E_h\lesssim\left(h^{r+1}|\boldsymbol{u}^E|_{r+1,\Omega_h}+h^{k+1/2}\|\boldsymbol{u}^E\|_{k+1,\infty,\Omega_h}\right)\|\boldsymbol{v}_h\|_{0,h}+\sum_{e\in\mathcal{E}_h^b}\langle\boldsymbol{v}_h\cdot\mathbf{n}_h,p^E-p_I\rangle_e.$$

From Lemma 4.6, it holds that

$$\sum_{e\in\mathcal{E}_h^b}\langle\boldsymbol{v}_h\cdot\mathbf{n}_h,p^E-p_I\rangle_e\lesssim\left(\sum_{e\in\mathcal{E}_h^b}h\|p^E-p_I\|_{0,e}^2\right)^{1/2}\|\boldsymbol{v}_h\|_{0,h}.$$

Finally, by the trace inequality in Lemma 2.1 and the approximation property of L^2-projection in Lemma 4.2, one obtains

$$\sum_{e\in\mathcal{E}_h^b}\langle \boldsymbol{v}_h\cdot \mathbf{n}_h, p^E-p_I\rangle_e \lesssim h^{t+1}|p^E|_{t+1,\Omega_h}\|\boldsymbol{v}_h\|_{0,h}.$$

Thus

$$E_h \lesssim \left(h^{k+1/2}\|\boldsymbol{u}^E\|_{k+1,\infty,\Omega_h}+h^{r+1}|\boldsymbol{u}^E|_{r+1,\Omega_h}+h^{t+1}|p^E|_{t+1,\Omega_h}\right)\|\boldsymbol{v}_h\|_{0,h}. \tag{35}$$

Combining (32)-(35) and Lemma 4.3, the theorem is proved. ☐

Corollary 5.1. *Assume $\delta \lesssim h^2$ holds, $r=t=l=k$. Let $(\boldsymbol{u},p)\in \boldsymbol{W}^{k+1,\infty}(\Omega)\cap \boldsymbol{H}^{k+1}(\Omega)\times H^{k+1}(\Omega)$ be the solution to Problem (1), $f\in H^k(\Omega)$ and $\boldsymbol{u}^E$, p^E are extended functions of $\boldsymbol{u}$ and p. Let $(\boldsymbol{u}_h,p_h)\in V_h\times Q_{0h}$ be the discrete solution of (13), then*

$$\begin{aligned}&\|\boldsymbol{u}^E-\boldsymbol{u}_h\|_{0,h}+\|p^E-p_h\|_{1,h}\\ \lesssim& h^{k+1}\left(\|\boldsymbol{u}\|_{k+1,\Omega}+\|p\|_{k+1,\Omega}+\|f\|_{k,\Omega}\right)+h^{k+1/2}\|\boldsymbol{u}^E\|_{k+1,\infty,\Omega_h}.\end{aligned}$$

Theorem 5.2. *Under the same assumption of Theorem 5.1, for $s:=\min\{r,t,k\}$, one gets*

$$\|\boldsymbol{u}^E-\boldsymbol{u}_h\|_{0,\Omega_h}\lesssim h^{s+1}(|\boldsymbol{u}|_{r+1,\Omega}+|p|_{t+1,\Omega})+h^{k+1/2}\|\boldsymbol{u}^E\|_{k+1,\infty,\Omega_h}+\delta^{k+1}h^{-\frac{1}{2}}M_{k+1}(\boldsymbol{u}^E),$$

$$\|\nabla(p-p_h)\|_{0,\mathcal{T}_h}\lesssim h^{s}(|\boldsymbol{u}|_{r+1,\Omega}+|p|_{t+1,\Omega})+h^{k+1/2}\|\boldsymbol{u}^E\|_{k+1,\infty,\Omega_h}+\delta^{k+1}h^{-\frac{1}{2}}M_{k+1}(\boldsymbol{u}^E).$$

Proof. Using the triangle inequality and the approximation error of interpolation in Lemma 4.1 yields

$$\begin{aligned}\|\boldsymbol{u}^E-\boldsymbol{u}_h\|_{0,\Omega_h}&\le\|\boldsymbol{u}^E-\boldsymbol{u}_I\|_{0,\Omega_h}+\|\boldsymbol{u}_I-\boldsymbol{u}_h\|_{0,\Omega_h}\\&\lesssim h^{r+1}|\boldsymbol{u}^E|_{r+1,\Omega_h}+\|\boldsymbol{u}_I-\boldsymbol{u}_h\|_{0,h},\end{aligned}$$

and the approximation error of L^2 projection in Lemma 4.2 implies

$$\begin{aligned}\|\nabla(p^E-p_h)\|_{0,\mathcal{T}_h}&\le\|\nabla(p^E-p_I)\|_{0,\mathcal{T}_h}+\|\nabla(p_I-p_h)\|_{0,\mathcal{T}_h}\\&\lesssim h^{t}|p^E|_{t+1,\Omega_h}+\|p_I-p_h\|_{1,h},\end{aligned}$$

then, combining Theorem 5.1 and Lemma 4.3, we obtain this proof. ☐

Remark 5.1. *Under the assumption $\delta\lesssim h^2$, Theorem 5.2 demonstrates a suboptimal convergence rate for the velocity field in the L^2-norm and an optimal order of convergence for the pressure field in the H^1-norm. From Tab. 1, it is observed that the velocity error estimate is $O(h^{k+1/2})$ for $s=k$.*

TABLE 1. *The error order of terms in L^2-norm under the assumption $\delta\lesssim h^2$.*

s	h^{s+1}	k	$h^{k+1/2}$	$\delta^{k+1}h^{-\frac{1}{2}}$	l	δ^l
1	h^2	1	$h^{1.5}$	$h^{3.5}$	1	h^2
2	h^3	2	$h^{2.5}$	$h^{5.5}$	2	h^4
3	h^4	3	$h^{3.5}$	$h^{7.5}$	3	h^6

Remark 5.2. *When boundary correction is not applied, discrepancy between the normal vector of the curved boundary and its polygonal approximation necessitates modification of the interpolation scheme (9), resulting in order reduction of the approximation error, which has been numerically validated.*

6. Numerical experiment

In this section, we test three examples to validate error results of the original mixed element method, without any boundary correction, and the correction method (13). Consider the Darcy problem on a circular domain $\{(x,y) : x^2+y^2 \leq 1\}$ and a ring domain $\{(x,y) : 1/4 \leq x^2+y^2 \leq 1\}$ with triangular meshes. Let $\boldsymbol{\nu}_h$ be the unit outward normal vector $\mathbf{n}$ on the curved boundary Γ. Before giving the numerical results, we define errors

$$e_u = \|\boldsymbol{u} - \boldsymbol{u}_h\|_{0,\Omega_h}, \qquad e_p = \|\nabla(p-p_h)\|_{0,\mathcal{T}_h}.$$

According to Remark 5.2 and Theorem 5.2, we expect to have a loss of accuracy for the original mixed element method, a suboptimal $O(h^{k+1/2})$ convergence for the correction method.

Example 1. Considering the problem (1) with solution

$$\boldsymbol{u}(x,y) = \begin{pmatrix} x^3(3x^2+2y^2-3) \\ x^4y \end{pmatrix}, \qquad p(x,y) = -\frac{1}{2}x^6 - \frac{1}{2}x^4y^2 + \frac{3}{4}x^4 - \frac{3}{64},$$

which satisfies a homogeneous Neumann boundary condition $\boldsymbol{u}\cdot\mathbf{n} = 0$ on Γ and $\int_\Omega p \, \mathrm{d}x = 0$.

Example 2. The exact solution is

$$\boldsymbol{u}(x,y) = \begin{pmatrix} 2\pi\cos(2\pi x)\sin(2\pi y) \\ 2\pi\sin(2\pi x)\cos(2\pi y) \end{pmatrix}, \qquad p(x,y) = -\sin(2\pi x)\sin(2\pi y),$$

which satisfies a non-homogeneous Neumann boundary condition $\boldsymbol{u}\cdot\mathbf{n} \neq 0$ on Γ and $\int_\Omega p \, \mathrm{d}x = 0$.

Example 3. The exact solution is

$$\boldsymbol{u}(x,y) = \begin{pmatrix} \pi\cos(\pi x)(e^y - e^{-y}) \\ \pi\sin(\pi x)(e^y + e^{-y}) \end{pmatrix}, \qquad p(x,y) = -(e^y - e^{-y})\sin(\pi x),$$

which satisfies a non-homogeneous Neumann boundary condition $\boldsymbol{u}\cdot\mathbf{n} \neq 0$ on Γ and $\int_\Omega p \, \mathrm{d}x = 0$.

We first present the results using the above tree examples to test the discrete scheme (13) on a circle domain and a ring domain. Results of boundary value correction are shown in Tabs 2-7. We observe an $O(h^{k+1/2})$ convergence in L^2-norm for velocity and an $O(h^k)$ convergence for pressure in H^1-norm, which agrees well with Theorem 5.2. Tab. 6 shows that some examples may exhibit a superconvergence error for velocity in L^2-norm.

TABLE 2. *Errors of Example 1 for velocity with boundary value correction on circle domain.*

h	$k=1$		$k=2$		$k=3$	
	e_u	order	e_u	order	e_u	order
1/8	4.56e-03	–	2.17e-04	–	5.78e-06	–
1/16	1.38e-03	1.72	3.57e-05	2.60	4.86e-07	3.57
1/32	4.14e-04	1.74	5.62e-06	2.67	3.89e-08	3.64
1/64	1.23e-04	1.75	8.68e-07	2.69	3.06e-09	3.67

Table 3. *Errors of Example 1 for pressure with boundary value correction on circle domain.*

h	$k=1$		$k=2$		$k=3$	
	e_p	order	e_p	order	e_p	order
1/8	5.75e-02	–	7.14e-03	–	3.93e-04	–
1/16	2.98e-02	0.95	1.86e-03	1.94	5.04e-05	2.96
1/32	1.49e-02	1.00	4.67e-04	2.00	6.21e-06	3.02
1/64	7.38e-03	1.01	1.16e-04	2.00	7.71e-07	3.01

Table 4. *Errors of Example 2 for velocity with boundary value correction on circle domain.*

h	$k=1$		$k=2$		$k=3$	
	e_u	order	e_u	order	e_u	order
1/8	2.52e-02	–	1.15e-03	–	3.35e-05	–
1/16	7.37e-03	1.78	1.89e-04	2.60	2.81e-06	3.58
1/32	2.14e-03	1.78	2.99e-05	2.66	2.22e-07	3.66
1/64	6.22e-04	1.78	4.59e-06	2.70	1.72e-08	3.69

Table 5. *Errors of Example 2 for pressure with boundary value correction on circle domain.*

h	$k=1$		$k=2$		$k=3$	
	e_p	order	e_p	order	e_p	order
1/8	4.85e-01	–	3.19e-02	–	1.57e-03	–
1/16	2.43e-01	0.99	7.87e-03	2.02	1.95e-04	3.01
1/32	1.21e-01	1.01	1.92e-03	2.04	2.33e-05	3.06
1/64	5.89e-02	1.04	4.59e-04	2.06	2.69e-06	3.12

Table 6. *Errors of Example 3 for velocity with boundary value correction on ring domain.*

h	$k=1$		$k=2$		$k=3$	
	e_u	order	e_u	order	e_u	order
1/8	4.77e-02	–	1.15e-03	–	1.50e-05	–
1/16	1.55e-02	1.54	1.83e-04	2.65	8.55e-07	4.13
1/32	5.25e-03	1.48	3.06e-05	2.58	5.02e-08	4.09
1/64	1.81e-03	1.45	5.26e-06	2.54	2.92e-09	4.02

Table 7. *Errors of Example 3 for pressure with boundary value correction on ring domain.*

h	$k=1$		$k=2$		$k=3$	
	e_p	order	e_p	order	e_p	order
1/8	4.33e-01	–	2.26e-02	–	7.78e-04	–
1/16	2.18e-01	0.99	5.66e-03	2.00	9.81e-05	2.99
1/32	1.09e-01	1.00	1.42e-03	2.00	1.23e-05	3.00
1/64	5.44e-02	1.00	3.54e-04	2.00	1.54e-06	3.00

As a comparison, we then solve the problem by standard Raviart-Thomas element method on two different domains, without any boundary value correction.

Tabs. 8-10 show an $O(h^{1/2})$ convergence in L^2-norm for velocity field when $k = 1, 2, 3$, which is a loss of accuracy, as expected.

TABLE 8. *Errors of Example 1 for velocity without boundary value correction on circle domain.*

h	$k=1$		$k=2$		$k=3$	
	e_u	order	e_u	order	e_u	order
1/8	7.26e-03	–	6.19e-03	–	6.14e-03	–
1/16	2.13e-03	1.77	1.79e-03	1.79	1.76e-03	1.81
1/32	6.11e-04	1.80	4.98e-04	1.84	4.83e-04	1.86
1/64	1.84e-04	1.73	1.45e-04	1.78	1.38e-04	1.81

TABLE 9. *Errors of Example 2 for velocity without boundary value correction on circle domain.*

h	$k=1$		$k=2$		$k=3$	
	e_u	order	e_u	order	e_u	order
1/8	2.86e-02	–	1.46e-02	–	1.39e-02	–
1/16	8.40e-03	1.77	4.88e-03	1.58	4.61e-03	1.59
1/32	2.53e-03	1.73	1.61e-03	1.60	1.51e-03	1.61
1/64	8.03e-04	1.66	5.45e-04	1.57	5.04e-04	1.58

TABLE 10. *Errors of Example 3 for velocity without boundary value correction on ring domain.*

h	$k=1$		$k=2$		$k=3$	
	e_u	order	e_u	order	e_u	order
1/8	6.57e-02	–	4.09e-02	–	3.64e-02	–
1/16	2.17e-02	1.60	1.42e-02	1.52	1.26e-02	1.53
1/32	7.49e-03	1.53	4.99e-03	1.51	4.42e-03	1.51
1/64	2.59e-03	1.53	1.76e-03	1.51	1.54e-03	1.52

7. Conclusion

In this paper, we analyze high-order Raviart-Thomas elements on domains with curved boundaries, employing weakly imposed Neumann boundary conditions in the variational formulation. Our analysis establishes a suboptimal convergence rate of $O(h^{k+1/2})$ for the velocity field in the L^2-norm and $O(h^k)$ for the pressure in the H^1-norm, which are numerically verified. Notably, without boundary correction, the convergence degrades to $O(h^{3/2})$ regardless of polynomial degree, highlighting the critical role of boundary correction. One fundamental limitation in our analysis stems from the discrepancy between the outward normal vectors of the exact boundary Γ and its discrete approximation Γ_h. This geometric inconsistency currently prevents the attainment of optimal convergence rates. Developing techniques to overcome this limitation constitutes a key objective for future work.

Acknowledgments

T. Zhao is supported by the National Natural Science Foundation of China (Grant No. 12171244), the National Natural Science Foundation of Henan Province (232300420350) and the Young Backbone Teachers Training Program of Zhongyuan University of Technology (2024XQG07).

References

[1] N. M. Atallah, C. Canuto, G. Scovazzi, The second-generation shifted boundary method and its numerical analysis, Computer Methods in Applied Mechanics and Engineering, 372:113341, 2020.

[2] N. M. Atallah, C. Canuto and G. Scovazzi, The high-order shifted boundary method and its analysis, Computer Methods in Applied Mechanics and Engineering, 394:114885, 2022.

[3] F. Bertrand, S. Munzenmaier and G. Starke. First-order system least squares on curved boundaries: Lowest-order Raviart-Thomas elements, SIAM Journal on Numerical Analysis, 52:880-894, 2014.

[4] F. Bertrand, S. Munzenmaier and G. Starke, First-order system least squares on curved boundaries: Higher-order Raviart-Thomas elements, SIAM Journal on Numerical Analysis, 52:3165-3180, 2014.

[5] F. Bertrand and G. Starke, Parametric Raviart-Thomas elements for mixed methods on domains with curved surfaces, SIAM Journal on Numerical Analysis, 54:3648-3667, 2016.

[6] D. Braess, Finite elements: theory, fast solvers, and applications in solid mechanics 3rd ed. Springer-Verlag, 2012.

[7] J. H. Bramble, T. Dupont and V. Thomée, Projection methods for Dirichlet's problem in approximating polygonal domains with boundary-value corrections, Mathematics of Computation 26:869-879, 1972.

[8] J. H. Bramble and J. T. King, A robust finite element method for nonhomogeneous Dirichlet problems in domains with curved boundaries, Mathematics of Computation 63:1-17, 1994.

[9] S. C. Brenner, Poincaré-Friedrichs inequalities for piecewise H^1 functions, SIAM Journal on Numerical Analysis, 41:306-324, 2003.

[10] S. C. Brenner and L. R. Scott, *The mathematical theory of finite element methods (third edition)*, Springer-Verlag, 1994.

[11] E. Burman, P. Hansbo and M. G. Larson, A cut finite element method with boundary value correction, Mathematics of Computation 87:633-657, 2018.

[12] E. Burman and R. Puppi, Two mixed finite element formulations for the weak imposition of the Neumann boundary conditions for the Darcy flow, Journal of Numerical Mathematics, 30:141-162, 2022.

[13] J. Cheung, M. Perego, P. Bochev and M. Gunzburger, Optimally accurate higher-order finite element methods on polytopial approximations of domains with smooth boundaries, Mathematics of Computation, 88:2187-2219, 2019.

[14] B. Cockburn, D. Gupta and F. Reitich, Boundary-conforming discontinuous Galerkin methods via extensions from subdomains, Journal of Scientific Computing, 42:144-184, 2009.

[15] B. Cockburn and M. Solano, Solving Dirichlet boundary-value problems on curved domains by extensions from subdomains, SIAM Journal on Scientific Computing 34:A497-A519, 2012.

[16] J. A. Cottrell, T. J. R. Hughes and Y. Bazilevs, Isogeometric Analysis: Toward Integration of CAD and FEA, John Wiley & Sons, Ltd., Chichester, 2009.

[17] C. D'Angelo and A. Scotti, A mixed finite element method for Darcy flow in fractured porous media with non-matching grids, ESAIM: Mathematical Modelling and Numerical Analysis 46:465-489, 2012.

[18] R. Durán, Mixed finite element methods, vol. 1939 of Lecture Notes in Mathematics, Springer-Verlag, Berlin, 1-44, 2008, lectures given at the C.I.M.E. Summer School held in Cetraro, June 26-July 1, 2006. Edited by D. Boffi and L. Gastaldi.

[19] G. Dziuk, Finite elements for the Beltrami operator on arbitrary surfaces, Lecture Notes in Mathematics, 1357:142-155, 1988. DOI:10.1007/BFb0082865.

[20] G. Dziuk, C. M. Elliott, Finite element methods for surface PDEs, Acta Numerica, 22(22):289-396, 2013.

[21] I. Ergatoudis, B. Irons and O. Zienkiewicz, Curved, isoparametric, quadrilateral elements for finite element analysis, International Journal of Solids and Structures, 4:31-42, 1968.

[22] G. N. Gatica, A simple introduction to the mixed finite element method theory and applications, Springer Briefs in Mathematics, 2014.

[23] T. J. R. Hughes, J. A. Cottrell and Y. Bazilevs, Isogeometric analysis: CAD, finite elements, NURBS, exact geometry and mesh refinement, Computer Methods in Applied Mechanics and Engineering, 194:4135-4195, 2005.

[24] Y. Hou, Y. Liu, and Y. Wang, A high-order shifted boundary virtual element method for Poisson equations on 2D curved domains, Journal of Scientific Computing, 99:85, 2024.

[25] M. Juntunen and R. Stenberg, Nitsche's method for general boundary conditions, Mathematics of Comoutation, 78:1353-1374, 2009.

[26] C. Lehrenfeld, T. V. Beeck and I. Voulis, Analysis of divergence-perserving unfitted finite element method for the mixed Poisson problem, arXiv:2306.12722.

[27] M. Lenoir, Optimal isoparametric finite elements and error estimates for domains involving curved boundaries, SIAM Journal on Numerical Analysis, 23:562-580, 1986.

[28] Y. Liu, W. Chen and Y. Wang, A weak Galerkin mixed finite element method for second order elliptic equations on 2D curved domains, Communications in Computational Physics, 32:1094-1128, 2022.

[29] A. Main and G. Scovazzi, The shifted boundary method for embedded domain computations. Part I: Poisson and Stokes problems, Journal of Computational Physics, 372:972-995, 2018.

[30] S. Pande, P. Papadopoulos and I. Babuška, A cut-cell finite element method for Poisson's equation on arbitrary planar domains, Computer Methods in Applied Mechanics and Engineering, 383:113875, 2021.

[31] R. Puppi, A cut finite element method for the Darcy problem, Preprint arXiv:2111.09922.

[32] E. M. Stein, Singular integrals and differentiability properties of functions, Princeton University Press, 2, 1970.

[33] G. Strang and A. E. Berger, The change in solution due to change in domain, Partial Differential Equations (D. C. Spencer, ed.), Proc. Sympos. Pure Math., vol. 23, Amer. Math. Soc, Providence, RI, 199-205, 1973.

[34] V. Thomée, Polygonal domain approximation in Dirichlet's problem, Ima Journal of Applied Mathematics, 11:33-44, 1973.

[35] V. Thomée, Approximate solution of Dirichlet's problem using approximating polygonal domains, Topics in Numerical Analysis (J. J. H. Miller, ed.), Academic Press, New York, 311-328, 1973.

[1] School of Science, Jiangsu University of Science and Technology, Zhenjiang 212003, Jiangsu, China.

E-mail: `ylhou@just.edu.cn`

[2] School of Mathematics and Information Science, Zhongyuan University of Technology, Zhengzhou 450007, Henan, China.

E-mail: `7043@zut.edu.cn and zhaotengjin@foxmail.com`